THE JOURNAL OF BIOLOGICAL CHEMISTRY VOL. 291, NO. 15, pp. 8162–8172, April 8, 2016

Identification of an Extracellular Gate for the Proton-coupled Folate Transporter (PCFT-SLC46A1) by Cysteine Cross-linking*

Received for publication, September 22, 2015, and in revised form, February 9, 2016 Published, JBC Papers in Press, February 16, 2016, DOI 10.1074/jbc.M115.693929

Rongbao Zhao[‡§], Mitra Najmi[‡], Andras Fiser[¶], and I. David Goldman[‡§1]**

*From the Departments of [‡]Molecular Pharmacology, [§]Medicine, [¶]Biochemistry, and **Systems and Computational Biology, Albert Einstein College of Medicine, Bronx, New York 10461*

The proton-coupled folate transporter (PCFT, SLC46A1) is required for intestinal folate absorption and folate homeostasis in humans. A homology model of PCFT, based upon the *Escherichia coli* glycerol 3-phosphate transporter structure, predicted that PCFT transmembrane domains (TMDs) 1, 2, 7, and 11 form an extracellular gate in the inward-open conformation. To assess this model, five residues (Gln^{45}-TMD1, Asn^{90}-TMD2, Leu^{290}-TMD7, Ser^{407}-TMD11 and Asn^{411}-TMD11) in the predicted gate were substituted with Cys to generate single and nine double mutants. Transport function of the mutants was assayed in transient transfectants by measurement of [^{3}H]substrate influx as was accessibility of the Cys residues to biotinylation. Pairs of Cys residues were assessed for spontaneous formation of a disulfide bond, induction of a disulfide bond by oxidization with dichloro(1,10-phenanthroline)copper (II) (CuPh), or the formation of a Cd^{2+} complex. The data were consistent with the formation of a spontaneous disulfide bond between the N90C/S407C pair and a CuPh- and Cd^{2+}-induced disulfide bond and complex, respectively, for the Q45C/L290C and L290C/N411C pairs. The decrease in activity induced by cross-linkage of the Cys residue pairs was due to a decrease in the influx V_{max} consistent with restriction in the mobility of the transporter. The presence of folate substrate decreased the CuPh-induced inhibition of transport. Hence, the data support the glycerol 3-phosphate transporter-based homology model of PCFT and the presence of an extracellular gate formed by TMDs 1, 2, 7, and 11.

Mammals meet their biosynthetic needs for one-carbon donors by absorption of dietary folates mediated by the proton-coupled folate transporter (PCFT)[2] (SLC46A1) (1, 2). Mutations in the PCFT gene that result in loss of the protein or its function are the basis for hereditary folate malabsorption (OMIM 229050), a rare autosomal recessive disorder (1, 3). PCFT transports protons along with folates as reflected in the current and acidification accompanying folate transport in oocytes that express this transporter (1, 4–6). Structure-function studies, based on site-directed and random mutagenesis, have begun to define residues and domains that play a key role in PCFT function. Elucidation of the secondary structure of PCFT, along with the residues that contribute to the aqueous translocation pathway, have been documented by the substituted cysteine accessibility method (7). The protein consists of 12 transmembrane helices, divided in half by a large intracellular loop, with C and N termini oriented into cytoplasm (8–10). Residues critical to folate/antifolate binding, proton coupling, and proton binding have been identified (5, 11–13). The roles of residues in the 2nd, 4th transmembrane domains (TMDs), and the loop connecting the 2nd and 3rd TMDs have been studied (14, 15). Analyses of the functional defects that occur in subjects with hereditary folate malabsorption have provided insights into residues important to PCFT protein folding, stability, and/or trafficking to the cell membrane, substrate binding, and oscillation of the carrier between its conformational states (13, 16–20).

PCFT expression is limited to eukaryotes; there are no closely related proteins present in archaea or bacteria, so that a high-resolution x-ray crystal structure with a high level of sequence identity is not available that would facilitate a structure/function analysis of the human or rodent proteins. Rather, homology modeling has identified the structure of the bacterial homolog, the glycerol-3-transporter, GlpT, as having a protein structure most like PCFT despite a low (14%) sequence identity (5, 10, 21). In this model, the transporter is in a conformation that is closed to the outside and open to the inside. According to the alternative access model, PCFT oscillates between this conformation and a conformation that is closed to the inside and open to the outside. This computational model has been used for correlation with functional data and for structural predictions as in the current study (5, 12–14, 21, 22).

In this inward facing homology model of PCFT, TMD-1, -2, -7, and -11 are predicted to cluster together in proximity to the extracellular interface to form an extracellular gate. To confirm the presence of such a gate, Cys pairs predicted to be in proximity were introduced into these TMDs at locations near the extracellular surface. The possibility that the pairs are sufficiently close to be cross-linked and/or form a complex was evaluated by assessment of function, which should be decreased when the mobility of the gate is restricted and the rate of oscil-

* This work was supported by National Cancer Institute, National Institutes of Health Grant CA082621. The authors declare that they have no conflicts of interest with the contents of this article. The content is solely the responsibility of the authors and does not necessarily represent the official views of the National Institutes of Health.

[1] To whom correspondence should be addressed: 1300 Morris Park Ave., Bronx, NY 10461. Tel.: 718-430-2302; Fax: 718-430-8550; E-mail: i.david.goldman@einstein.yu.edu.

[2] The abbreviations used are: PCFT, proton-coupled folate transporter; CuPh, dichloro(1,10-phenanthroline)copper(II); GlpT, glycerol-3-phosphate transporter; MTSEA biotin, 2-((biotinoyl)amino)ethyl methanethiosulfonate; MTX, methotrexate; TMD, transmembrane domain; DSL, disulfide bond-less.

lation of the carrier is suppressed, under three conditions: (i) spontaneous formation of a disulfide bond accompanied by diminished accessibility of Cys residues to a biotinylation reagent, (ii) disulfide bond formation induced by oxidation with CuPh, and (iii) complex formation between a Cd^{2+} ion and two Cys-substituted residues. In this way, evidence was obtained to indicate that pairs of Cys-substituted residues were cross-linked or complexed involving all of the predicted 1, 2, 7, and 11 TMDs. The data are consistent with the proximity of these residues and an external gate comprised involving these TMDs that controls access to the aqueous translocation pathway of this transporter.

Experimental Procedures

Cells and Culture Conditions—R1–11 cells were derived from HeLa cells and express neither the reduced folate carrier, due to deletion of its gene, nor PCFT due to methylation of its gene promotor (23, 24). R1–11 cells were maintained in RPMI 1640 medium supplemented with 10% fetal bovine serum, 100 units/ml of penicillin, and 100 μg/ml of streptomycin. R1–11 cells were thawed regularly (once every 3 months) from liquid nitrogen stocks to ensure that PCFT expression was absent (25).

Key Chemicals—[3′,5′,7-^{3}H]MTX and generally labeled [^{3}H]pemetrexed were obtained from Moravek Biochemicals (Brea, CA). MTSEA biotin and EZ-Link Sulfo-NHS-LC-Biotin were purchased from Biotium (Hayward, CA) and Thermo Scientific (Rockford, IL), respectively. DL-Dithiothreitol (DTT) was obtained from MP Biochemicals (Solon, OH), dichloro (1,10-phenanthroline)copper(II) (CuPh) was from Santa Cruz Biotechnology, and cadmium chloride was purchased from Fisher Scientific (Pittsburg, PA).

Site-directed Mutagenesis—An engineered human PCFT, which harbors two point mutations (C66S and C298S) and is tagged with HA (hemagglutinin) at the C terminus, was used as a template for site-directed mutagenesis in most cases. In some cases, HA-tagged, Cys-less PCFT was also used for mutagenesis. A desired mutation was first introduced into the template using the QuikChange II Site-directed Mutagenesis Kit (Stratagene, La Jolla, CA). After sequence verification, a second mutation was introduced into PCFT in a similar way to generate double mutants. Automated sequencing was performed in the Albert Einstein Cancer Center Genomics Shared Resource.

Transient Transfection—R1–11 cells were used as recipients for all transient transfections. For transport studies, cells were seeded in 20-ml Low Background glass scintillation vials (Research Products International Corporation, Prospect, IL). For biotinylation studies, cells were seeded in 6-well plates. In both cases, transfections were performed with Lipofectamine 2000 (Invitrogen) according to the manufacturer's protocol 2 or 3 days after seeding cells. Transport and biotinylation assays were always performed 2 days after transfection. Cell growth medium was refreshed 1 day after transfection.

Membrane Transport—Cells were washed twice with HBS (HEPES-buffered saline: 20 mM HEPES, 5 mM dextrose, 140 mM NaCl, 5 mM KCl, 2 mM $MgCl_2$, pH 7.4) and incubated in the same buffer at 37 °C for 20 min. The incubation buffer was then removed and transport was initiated by the addition of 0.5 ml of pre-warmed (37 °C) MBS (MES-buffered saline: 20 mM MES, 5 mM dextrose, 140 mM NaCl, 5 mM KCl, 2 mM $MgCl_2$, pH 5.5) containing 0.5 or 50 μM[^{3}H]MTX. For [^{3}H]pemetrexed influx studies, transport was initiated by addition 0.5 ml of pre-warmed (37 °C) HBS containing 1 μM drug and halted after 1 min by the addition of 5 ml of ice-cold HBS. Cells were washed three times with ice-cold HBS and digested in 0.5 ml of 0.2 M NaOH at 65 °C for 1 h. Radioactivity in 0.4 ml of lysate was measured on a liquid scintillation spectrometer and normalized to the protein level obtained with the BCA Protein Assay (Pierce). All transport assays were performed at least three times on separate days. In each experiment every data point was conducted in duplicate.

Analysis of PCFT at the Cell Surface and Accessibility of PCFT Cys Residues by Biotinylation—Although biotinylation of Lys residues detects the level of PCFT at the plasma membrane, Cys biotinylation with a membrane impermeant reagent determines the accessibility of a Cys residue to the extracellular milieu (7, 9, 10, 14). For surface labeling, cells were treated with EZ-Link Sulfo-NHS-LC-Biotin at a concentration of 1 mg/ml in HBS. For Cys biotinylation, cells were treated with MTSEA biotin at a concentration of 0.2 mg/ml in HBS. Both treatments were performed at room temperature for 30 min. Following this, processing of both biotinylation reactions was identical. Cells were washed in HBS at room temperature, then overlaid on ice with 0.7 ml of hypotonic buffer (0.5 mM Na_2HPO_4, 0.1 mM EDTA, pH 7.0) containing protease inhibitor mixture (Roche Applied Science). The cells were then detached from the plates with a disposable cell lifter and centrifuged at 16,000 × *g* for 10 min at 4 °C. The pellet was resuspended in 0.4 ml of lysis buffer (50 mM Tris base, 150 mM NaCl, 1% Nonidet P-40, 0.5% sodium deoxycholate, pH 7.4) and a 50-μl portion was collected as a sample from crude membranes and stored at −20 °C. The remaining suspension was mixed on a rotisserie for 0.5 to 1 h and centrifuged at 16,000 × *g* for 15 min, all at 4 °C. The supernatant was mixed on a rotisserie overnight at 4 °C with 50 μl of streptavidin-agarose beads (Fisher Scientific) that had been pre-washed three times with the lysis buffer. The agarose beads were then washed at room temperature twice with the lysis buffer and then an additional two times with the lysis buffer containing 2% SDS, each with a 20-min mixing on a rotator. The precipitated proteins were then released from the beads by heating at 95 °C for 5 min in 2× SDS-PAGE sample loading buffer with or without DTT.

Protein samples were resolved on standard 12.5% SDS-PAGE. The precipitated proteins released into the sample buffer were loaded directly on gels, whereas the crude membrane fractions were mixed (1:1) with the 2× SDS-PAGE sample loading buffer at room temperature before loading on the gels. After SDS-PAGE, proteins were transferred to an Immobilon-P Transfer Membrane (Millipore, Billerica, MA) and blocked with 10% dry milk in TBST (20 mM Tris, 135 mM NaCl, 1% Tween 20, pH 7.6) overnight at 4 °C. The blots were probed either with polyclonal anti-HA antibody (H6908) (Sigma, 1:4,000 in TBST, 0.1% milk) or monoclonal anti-β-actin antibody (A5441) (Sigma, 1:10,000 in TBST, 0.1% milk) and then a second antibody, anti-rabbit, or anti-mouse IgG-HRP conjugate (Cell Signaling Technology, 1:5000 in TBST), respectively.

The blots were developed with Western Lightning Plus-ECL (PerkinElmer Life Sciences, Waltham, MA).

Reduction, Oxidation, or Complex Formation of PCFT Expressed in Cells—Reduction with DTT, oxidation with CuPh, and complex formation with $CdCl_2$ were all performed in transient transfectants expressing PCFT mutants immediately before transport or biotinylation assays. For reduction with DTT, cells were washed once with HBS at room temperature and then incubated for 10 min at room temperature with freshly made 12 mM DTT in HBS. After cells were washed twice with HBS at room temperature, transport or Cys accessibility was assessed. The control for DTT reduction was cells treated with HBS that did not contain DTT. For oxidation with CuPh, DTT-treated cells were washed a third time with ice-cold HBS then incubated for 5 min on ice with 10 μM CuPh, which was prepared before experiments by a 1 to 1000 dilution of a frozen stock (a mixture of 10 mM dichloro(1,10-phenanthroline)copper(II) and 3 mM $CuSO_4$ in water) in ice-cold HBS. The cells were washed four times with ice-cold HBS prior to assessment of transport. The control for CuPh treatment was cells exposed to CuPh-free HBS. For complex formation with Cd^{2+}, cells were treated with DTT then washed twice with HBS as indicated above, then exposed to $CdCl_2$ (8 μM) in HBS for 20 min at 37 °C. The buffer was then aspirated and transport was assessed in HBS containing 8 μM $CdCl_2$. For a control, no cadmium was present in the preincubation or transport buffer.

Oxidative Cross-linkage in the Presence of Folic Acid—Transient transfectants were washed once with HBS and incubated with 12 mM DTT in HBS for 10 min at room temperature. The cells were washed three times with HBS, incubated with 1.7 mM folic acid in HBS (1 ml) for 1 min, all at room temperature, then cooled in an ice water bath for 5 min. A CuPh solution in HBS (2.5 μM, 1 ml) at 0 °C was added to the cells to achieve a final CuPh concentration of 1.25 μM and a final folic acid concentration of 0.85 mM, and the incubation continued for 5 min at this temperature. The cells were then washed three times with ice-cold HBS and placed in a 37 °C water bath for 1 min following which MTX influx was initiated with the addition of 0.5 ml pre-warmed MBS (pH 5.5) containing 0.5 μM [^{3}H]MTX.

Statistical Analysis—Statistical analyses were conducted with analysis of variance, GraphPad Software (La Jolla, CA).

Homology Model of Human PCFT—A comparative protein structure model for PCFT has been built for the interpretation of experimental observations within a three-dimensional context. A variety of homology models that differed in their target-to-template input alignments were built and the Prosa energy score evaluated (26). The most stable model was obtained using input from the HHpred method (27), a hidden Markov model-based fold-recognition and alignment method. The best-scoring template found was the crystal structure of GlpT from *Escherichia coli* (Protein Data Bank code 1pw54), as in other studies (5, 10, 12–14, 21, 22). The optimal sequence alignment between PCFT and 1pw54 served as input for the comparative protein structure modeling program MMM (28–31). The resulting model underwent additional quality verification by cross-correlating the location of predicted transmembrane helical segments using HMMTOP (32) with the ones observed in the model. The corresponding models resulted in a largely conserved core of transmembrane segments, but there were substantial variations in the modeling of the extra- and intracellular loop regions.

Results

Identification of Candidate Residues Predicted to Form an Extracellular Gate for the Substrate Translocation Pathway in Human PCFT—A homolog model has been built for human PCFT based upon the crystal structure of the *E. coli* GlpT transporter. As indicated in Fig. 1, TMD1, -2, -7, and -11 are predicted to be in a position to form a gate at the entry pathway for substrate in an outward-closed, inward-opened, conformation. Gln^{45} in TMD1, Asn^{90} in TMD2, Leu^{290} in TMD7, Ser^{407}, and Asn^{411} in TMD11 are located in the termini of these TMDs and pairs are predicted to be in sufficient proximity to form disulfide bonds and/or a complex with Cd^{2+} when substituted with Cys residues.

Activity and Expression of Single and Double Cys PCFT Mutants—To investigate the dynamic interactions between and among these transmembrane helices, five single mutations (Q45C, N90C, L290C, S407C, and N411C) and nine double mutations (Q45C/N90C, Q45C/L290C, Q45C/S407C, Q45C/N411C, N90C/L290C, N90C/S407C, N90C/N411C, L290C/S407C, and L290C/N411C) were generated in a modified PCFT template in which both Cys^{66} and Cys^{298} residues were substituted with serine. The double mutant containing S407C and N411C was not studied because both mutations are located in the same helix. Previous studies demonstrated that Cys^{66} and Cys^{298} are the only residues that form a disulfide bond in the wild-type PCFT and this bond is not required for protein stability or function (9). The removal of these Cys residues eliminated the native disulfide bond in the molecule that would confound interpretation of the results but minimally affects function of the transporter. This template is identified as PCFT-DSL and these mutants are identified with a "-DSL" suffix (disulfide bond-less), indicating a platform that lacks this post-translational modification. The activity of PCFT-DSL was 72 ± 5% of that of wild-type PCFT assessed by [^{3}H]MTX influx (0.5 μM, pH 5.5) in transient transfectants based upon three independent experiments. A Cys-less PCFT (PCFT-CL), in which all Cys residues were converted to Ser was not routinely used to generate these mutants because introduction of additional mutations in the Cys-less scaffold often results in destabilization of the protein, whereas the same mutations generated in wild-type or DSL PCFT are expressed and functional, a phenomenon also observed for other transporters (33, 34).

The activity of the PCFT mutants was assessed in transient transfectants by measuring influx of [^{3}H]MTX at pH 5.5. As indicated in Fig. 2*A*, activities of the single mutants, N90C-DSL, S407C-DSL, and N411C-DSL were comparable with that of PCFT-DSL (91.8, 100, and 98.1%, respectively). Activity of Q45C-DSL was half, whereas activity of the L290C-DSL mutant was one-fourth that of PCFT-DSL. As discussed below, neither Q45C nor L290C forms a disulfide bond with another Cys residue in the molecule, but both were pre-modified with endogenous thiols. All the double mutants exhibited an activity ≤25% that of PCFT-DSL except the N90C/N411C mutant, which

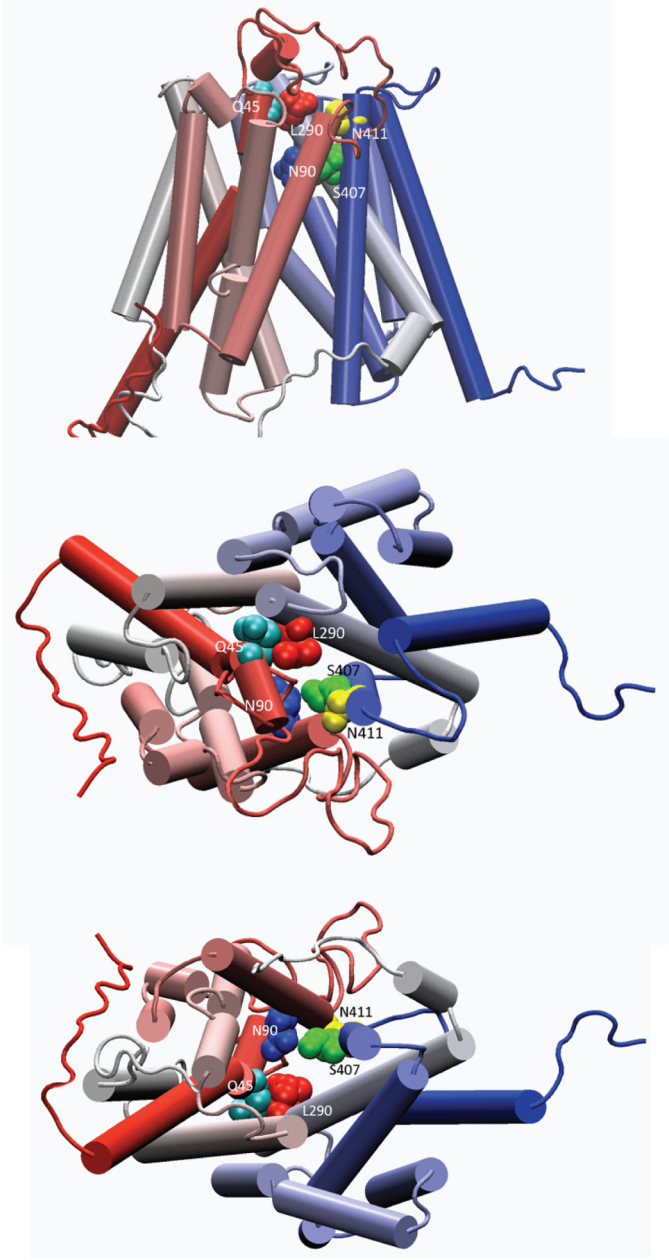

FIGURE 1. **A homology model of PCFT in the inward-open configuration.** The model, based upon homology to the GlpT transporter, predicts that TMD1, -2, -7, and -11 come together to form a gate at the extracellular interface of the aqueous translocation pathway. Residues that are potentially close enough to form a disulfide bond, or a complex with Cd^{2+}, when Cys substituted, are indicated: Gln^{45} (TMD1, *turquoise*), Asn^{90} (TMD2, *blue*), Leu^{290} (TMD7, *red*), Ser^{407} (TMD11, *green*), and Asn^{411} (TMD11, *yellow*). The *upper panel* is a lateral view. The *middle panel* is a view into the translocation pathway from the extracellular compartment. The *lower panel* is a view into the translocation pathway from the cytoplasm.

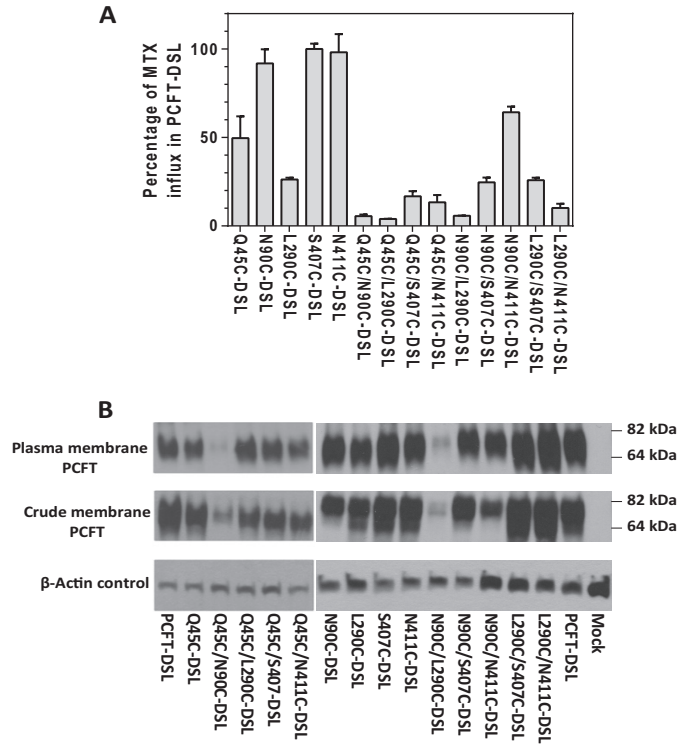

FIGURE 2. **Transport function and expression of human PCFT single and paired Cys mutants.** Mutant PCFTs were transfected into R1–11 (PCFT- and RFC-null) cells 2 days before function and expression were assessed. *Panel A*, activity of the PCFT mutants was determined by assessment of [^{3}H]MTX influx at 0.5 μM and pH 5.5 over 1 min and expressed as percentage of influx in PCFT-DSL, the scaffold for the mutants. Data are the mean ± S.E. from three independent experiments. *Panel B*, Western blot analysis of PCFT levels at the plasma membrane surface by biotinylation of Lys residues and in the crude membranes extract. Molecular markers are indicated on the *right*. β-Actin is the sample loading control. The images are representative of three independent analyses.

retained 64% of PCFT-DSL activity. The activity of most double mutants was much lower than what might be expected from their two single constituting mutants (*e.g.* 13% activity for the Q45C/N411C-DSL as compared with 50 and 98% for the Q45C-DSL and N90C-DSL mutants, respectively).

PCFT expression at the plasma membrane was measured by cell surface biotinylation with a reagent targeting free amine groups. The expression of all single mutants in the plasma membrane was comparable with that of PCFT-DSL (Fig. 2*B*). Although expression of the Q45C/N90C-DSL and N90C/L290C-DSL double mutants in the plasma membrane was markedly decreased, expression of the other double mutants was comparable with that of PCFT-DSL. Expression of all PCFT mutants in the crude membranes tended to mirror the cell surface expression suggesting that trafficking of the mutants to the cell membrane was largely intact. Hence, the single mutant, L290C-DSL and the double mutants, Q45C/L290C-DSL, Q45C/S407C-DSL, Q45C/N411C-DSL, N90C/S407C-DSL, L290C/S407C-DSL, and L290C/N411C-DSL, had markedly decreased activity despite their robust expression at the plasma membrane. The basis for the loss of activity of the Q45C/N90C-DSL and the N90C/L290C-DSL pairs was less clear because this could be related to their low levels of expression.

Impact of DTT Reduction on Transport Activities of the Mutants—To assess whether formation of a disulfide bond between two Cys-substituted residues in the double mutants was a basis for the reduction in PCFT function, all transient transfectants were treated with 12 mM DTT at room temperature and neutral pH for 10 min to break disulfide bonds before MTX influx was measured at acidic pH (35). As indicated in Fig. 3*A*, which illustrates the fold-increase in transport activity induced by DTT, this treatment had no significant effect on the activity of the N90C-DSL, S407C-DSL, and N411C-DSL single

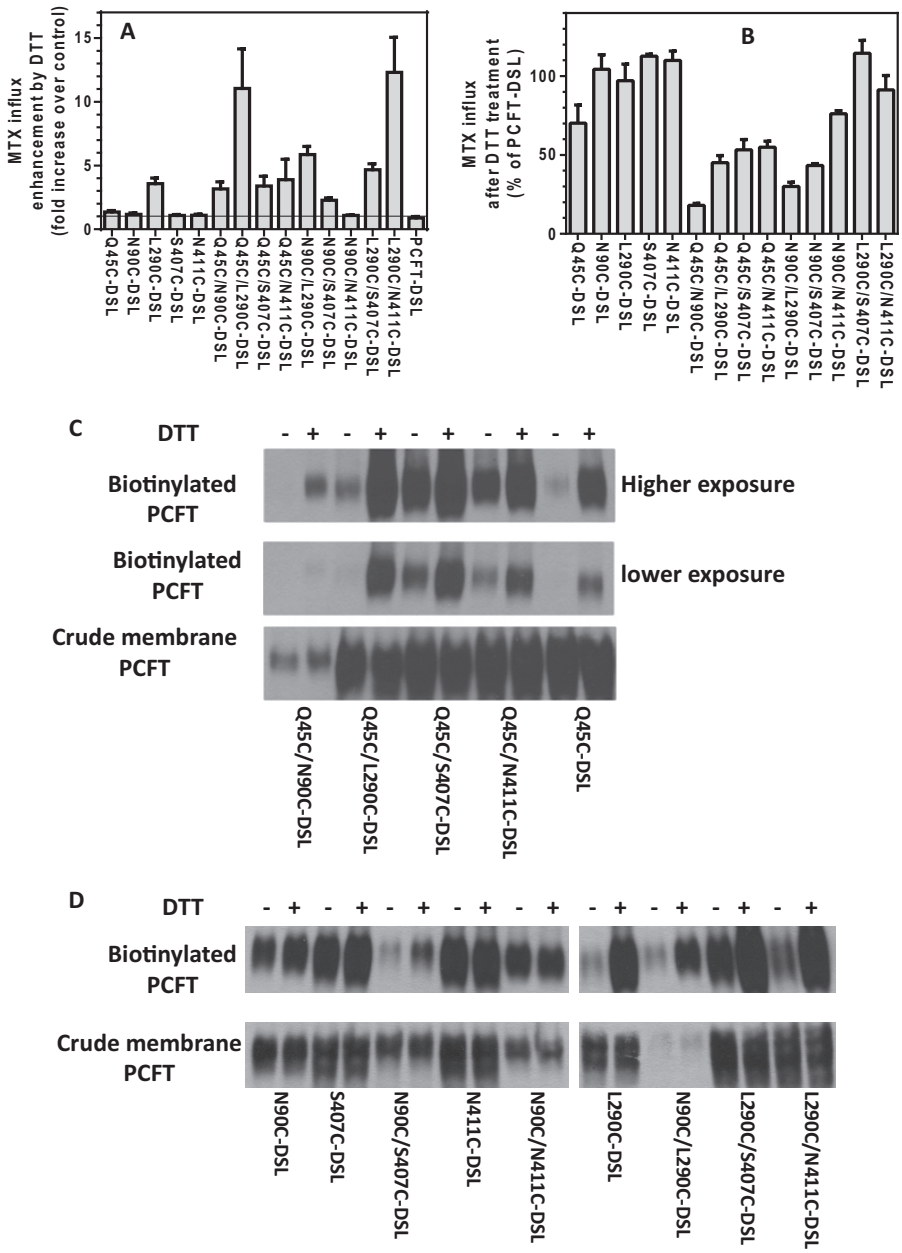

FIGURE 3. **Effect of DTT on the transport activity and accessibility of the Cys-substituted residues.** *Panel A*, transient transfectants were treated with 12 mM DTT at room temperature for 10 min. After the DTT solution was removed, the cells were washed twice with HBS at 0 °C before influx of [^{3}H]MTX (0.5 μM, pH 5.5, 37 °C, 1 min) was assessed. The controls were the cells treated only with HBS (lacking DTT). Data are expressed as fold-increase in MTX influx in the DTT-treated, as compared with the buffer alone treated, cells. *Panel B*, [^{3}H]MTX influx (0.5 μM, pH 5.5, 1 min) after DTT treatment as a percentage of DTT-treated PCFT-DSL cells set to 100%. Data are the mean ± S.E. from three independent experiments for both *panels A* and *B*. *Panels C* and *D*, accessibility of Cys-substituted residues probed with MTSEA biotin, a membrane-impermeant thio-reactive labeling reagent, with or without DTT treatment (12 mM, room temperature, 10 min). In *panel C*, two different exposures are shown to better illustrate the full range of band intensity. The film for the crude membrane PCFT was overexposed to allow visualization of the weak bands. The *vertical gap* between the images in *panel D* indicates two groups (left and right) run on two separate SDS gels but at the same time. The images are representative of two independent analyses.

mutants and the N90C/N411C-DSL double mutant or on the control PCFT-DSL. DTT produced a slight (35%, $p = 0.04$) increase in the activity of the Q45C-DSL mutant. However, DTT increased activity of the L290C-DSL mutant by a factor of 4 and increased the activities of the Q45C/N90C-DSL, Q45C/L290C-DSL, Q45C/S407C, Q45C/N411C-DSL, N90C/L290C-DSL, N90C/S407C-DSL, L290C/S407C-DSL, and L290C/N411C-DSL mutants by factors of 3.2, 11.0, 3.4, 3.5, 5.9, 2.3, 4.6, and 12.3, respectively, suggesting that the Cys residue(s) in these mutants were modified and these modifications were reversed by DTT. The fact that DTT had no impact on the function of N90C-DSL and S407C-DSL single mutants, but resulted in a greater than 2-fold augmentation of the activity of the N90C/S407C-DSL mutant, is consistent with the spontaneous formation of disulfide bond between these residues as suggested from the data in Fig. 2*A*. Similarly, a disulfide bond may have formed in the Q45C/N90C-DSL, Q45C/S407C-DSL, and Q45C/N411C double mutants because DTT produced a greater than 3-fold increase in the activities of these constructs but had only a slight effect on the activity of the single Q45C-

DSL mutant, and no effect on the activity of the N90C-DSL, S407C-DSL, and N411C-DSL single mutants.

Fig. 3*B* illustrates activities of the various mutants after DTT treatment as a percentage of function of DTT-treated PCFT-DSL. The activities of the single mutant L290C-DSL and the double mutants, L290C/S407C-DSL and L290C/N411C-DSL, were comparable with the activity of PCFT-DSL under these conditions, suggesting that these mutants are fully functional when the substituted Cys residue(s) are not modified. Although the activity of Q45C-DSL reached 70% of PCFT-DSL, the function of Q45C/L290C-DSL, Q45C/S407C-DSL, and Q45C/N411C-DSL was increased to ~50% of PCFT-DSL with DTT reduction. This degree of impaired function of the double mutants could be attributed to the decreased function of the Q45C single mutant even after DTT. The activities of Q45C/N90C-DSL and N90C/L290C-DSL were only 20 and 30%, respectively, of PCFT-DSL after DTT treatment despite the much lower level of expression, suggesting that these two mutants are also functional. Therefore, all these mutants exhibited sufficient intrinsic activity for further analysis.

Effect of DTT Reduction on the Accessibility of the Substituted Cys Residues—As previously noted, residues, Gln^{45}, Asn^{90}, Leu^{290}, Ser^{407}, and Asn^{411} of human PCFT are predicted to be located near the extracellular interface of the aqueous translocation pathway. If this is the case, then the single substituted Cys residues at these positions should be accessible to the extracellular compartment and modified by a membrane-impermeant sulfhydryl-targeting biotinylation reagent such as MTSES biotin. However, if the two Cys residues form a spontaneous disulfide bond in the double mutant, the labeling of each of the two residues will be diminished or eliminated as previously demonstrated for the native Cys^{66} and Cys^{298} residues of the wild-type human PCFT (9). On the other hand, if the disulfide bond is reduced by DTT, these two Cys residues should become available for labeling (9). Accordingly, accessibility of the substituted Cys residues in all mutants was assessed before and after DTT reduction with MTSES biotin. As indicated in Fig. 3, *C* and *D*, the substituted Cys residues in the N90C-DSL, S407C-DSL, and N411C-DSL single mutants were labeled to the same extent prior to, and after, DTT treatment consistent with the lack of effect of DTT on their transport activity (Fig. 3*A*). However, DTT markedly increased labeling of the Q45C-DSL and L290C-DSL single mutants and increased labeling of all double mutants, to different extents, except for the N90C/N411C-DSL mutant. The increase in accessibility of the N90C/S407C-DSL mutant with DTT, and the lack of increased accessibility for the N90C-DSL and S407C-DSL single mutants (Fig. 3*D*) was consistent with the presence of a spontaneous disulfide bond as was the loss of intrinsic activity of this double mutant (Fig. 2*A*). The lack of DTT-induced labeling of the N90C/N411C-DSL mutant suggested the lack of spontaneous formation of a disulfide bond, also consistent with the lack of a DTT effect on the activity of this mutant. Because DTT treatment resulted in labeling of the Q45C-DSL and L290C-DSL single mutants, no conclusion was possible as to whether a disulfide bond formed spontaneously in the double mutants harboring these Cys-substituted residues in which accessibility also increased with DTT. The biotinylation of the

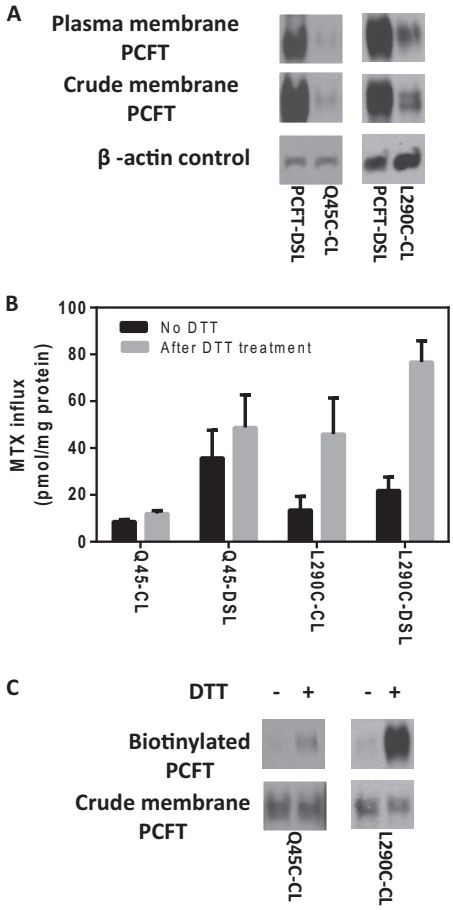

FIGURE 4. **Expression, transport activity, and accessibility of the Q45C and L290C mutants introduced into Cys-less PCFT or PCFT-DSL.** *Panel A*, expression of the Q45C-CL and L290C-CL mutations in a Cys-less (*CL*) or disulfide bond-less (*DSL*) scaffold at the plasma membrane and crude membrane extract. *Panel B*, impact of DTT treatment (12 mM, room temperature, 10 min) on activities of Q45C-CL and L290C-CL PCFT as compared with the Q45C-DSL and L290C-DSL mutants. Transport activities were based on [^{3}H]MTX influx (0.5 μM, pH 5.5, 37 °C, 1 min). Data are the mean ± S.E. from three independent experiments. *Panel C*, accessibility of the Cys residue in the Q45C-CL and L290C-CL mutants with or without reduction with DTT (12 mM, room temperature, 10 min). The images in *panels A* and *C* are representative of at least two independent analyses and the vertical gaps between images indicate that the films were from separate experiments.

substituted Cys residues in the S407C-DSL and N411C-DSL mutants, and the lack of biotinylation of the substituted Cys residue in the Q45C-DSL mutant in the absence of DTT treatment, were also observed for the same mutations introduced into Cys-less PCFT (10).

Post-translational Modifications of the Substituted Cys Residues in Q45C-DSL and L290C-DSL PCFT Mutants—As indicated above, DTT treatment enhanced both the activity and accessibility of the Q45C-DSL and L290C-DSL single mutants. To exclude the possibility that the substituted Cys in Q45C-DSL and L290C-DSL mutants spontaneously form a disulfide bond with one of the five remaining native Cys residues, the Q45C or L290C mutations were introduced in the Cys-less PCFT to generate the Q45C-CL and L290C-CL mutants. As indicated in Fig. 4*A*, expression of the Q45C-CL and L290C-CL mutants was much lower than that of PCFT-DSL both at the plasma membrane and in the crude membrane fractions. This is consistent with the previous finding that the Cys-less PCFT is

vulnerable to the introduction of additional mutations (15, 33). Consistent with the low expression, the activities of the Q45C-CL and L290C-CL mutants were lower than their counterparts in the DSL scaffold. However, the increase in activities of both mutants with DTT was comparable with the increase when generated in the DSL scaffold (Fig. 4*B*) and, most important, the accessibility of both mutants to biotinylation was increased after treatment with DTT in the Cys-less scaffold (Fig. 4*C*). Hence, the impact of DTT on the activities or accessibility of the substituted Cys residues was similar for the Q45C or L290C mutations regardless of the template used for the mutants (Cys-less *versus* disulfide bond-less). These results indicate that post-translational modification of the Cys-substituted residue in either Q45C-DSL or L290C-DSL is not due to the formation of a disulfide bond with one of the native Cys residues. Rather, the data are consistent with modification by endogenous thiols similar to what occurred when a Cys residue was substituted for Thr^{338} of the cystic fibrosis transmembrane conductance regulator (36). Most important, the modifications of Q45C and L290C mutants appeared to be reversible with DTT reduction.

The Impact of CuPh—DTT reduction not only restored activity of most single mutants and some double mutants as indicated in Fig. 3*B*, but also freed-up sulfhydryl groups for modification in the mutants. This enabled an analysis of the impact of CuPh, an agent that cross-links adjacent thiol groups. As indicated Fig. 5*A*, CuPh did not significantly alter the activity of the single mutants suggesting that CuPh neither non-specifically reduces PCFT function nor interferes with the function of the single Cys mutants. A critical factor in this assay was that the L290C-DSL mutant maintained its function after CuPh treatment in contrast to the 80% reduction in activity due to the post-translational modification (Figs. 2 and 3). This indicates that this Cys residue was not modified by CuPh treatment under these conditions. It can be seen that CuPh oxidation resulted in a significant decrease in the activities of all double mutants as compared with that of the single mutant constituents. The greatest reduction in activity induced by CuPh oxidation was observed in the Q45C/L290C-DSL (79%), N90C/S407C-DSL (85%), and L290C/N411C-DSL (89%) mutants.

The effect of CuPh oxidation on MTX influx kinetics was assessed for the Q45C/L290C-DSL, N90C/S407C-DSL, and L290C/N411C mutants at MTX concentrations of 0.5 and 50 μM, the latter >10 times greater than the influx K_t for wild-type PCFT (13), thereby reflecting the influx V_{max} (Table 1). Based upon three experiments, oxidation by CuPh reduced activity of the Q45C/L290C-DSL mutant by 54% at 50 μM, comparable with 64% at 0.5 μM MTX. Similarly, CuPh oxidation reduced activity of the N90C/S407C-DSL mutant by 87% at 50 μM, comparable with 84% at 0.5 μM MTX, and decreased activity of the L290C/N411C-DSL mutant by 92% at 50 μM, comparable with 88% at 0.5 μM MTX. Hence, the major impact of CuPh oxidation appears to be a reduction in the influx V_{max} for both mutants, consistent with an alteration in the mobility of the carrier.

The Impact of Cadmium Chloride—Cd^{2+} interacts with the sulfhydryl group of two Cys residues to form a complex and the extent of this interaction depends upon the proximity of the residues (37). Cd^{2+} has been used to probe the proximity of Cys residues in sodium channels and neuronal glutamate transporters (35, 37). Fig. 5*B* indicates the effect of Cd^{2+} following DTT treatment on the activity of the mutants. This was performed at neutral pH to preserve the capacity of Cd^{2+} to form a complex with Cys residues, which is much weaker at pH 5.5 (see below). Activity was determined with pemetrexed because this agent retains greater influx activity at neutral pH than MTX (38, 39). Cd^{2+} had no effect on the activity of any of the single mutants nor did it significantly decrease the activity of the Q45C/L290C-DSL and N90C/L290C double mutants as compared with their respective constituting single mutants. However, Cd^{2+} significantly reduced the activities of all other double mutants as compared with the respective constituting single mutants. Hence, except for the Q45C/L290C pair, the effect of Cd^{2+} was consistent with the effect of CuPh oxidation, with the

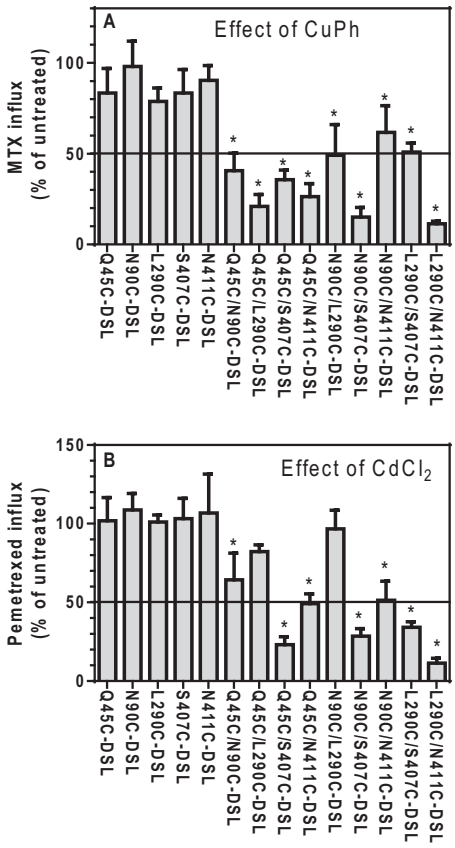

FIGURE 5. **Effect of oxidation by CuPh, or Cd^{2+} complex formation, on transport activities of PCFT mutants.** Transient transfectants were incubated with DTT (12 mM) at room temperature for 10 min and washed before assessing the effect of CuPh or Cu^{2+} treatment. *Panel A*, the impact of CuPh oxidation was assessed after incubating cells with 10 μM CuPh in HBS at 0 °C for 5 min. The cells were then washed four times with ice-cold HBS before [^{3}H]MTX influx was measured (0.5 μM, pH 5.5, 37 °C, 1 min). Controls for each mutant transfectants were subjected to identical treatment except for the omission of CuPh. The graph is [^{3}H]MTX influx as a percentage of influx in cells not exposed to CuPh oxidation (untreated) indicated as 100%. Data are the mean ± S.E. from four independent experiments. *Panel B*, the impact of Cd^{2+} on transport function. PCFT activity was assessed with [^{3}H]pemetrexed influx (1 μM, pH 7.4, 37 °C, 1 min). Cd^{2+} (8 μM) was present in both the preincubation and transport buffer at pH 7.4. Cd^{2+} was neither in the preincubation nor in the transport buffer for the control (untreated). Data are the mean ± S.E. from three independent experiments. The *asterisk* indicates that the decrease in transport activities of the double mutants was statistically significant as compared with cells that express the respective single mutants.

TABLE 1

Impact of CuPh oxidation on MTX influx at low (below saturation) and high (saturating) substrate concentrations

[^{3}H]MTX influx is expressed in units of pmol/mg of protein/min. The cells expressing the mutants were treated with DTT, washed, oxidized by CuPh, and washed again before assessing MTX influx at pH 5.5, 37 °C over 1 min. The data are the mean ± S.E. from three independent experiments.

Mutant	MTX	MTX influx not oxidized	MTX influx CuPh-oxidized	Ratio oxidized/not oxidized
	μM			
Q45C/L290C-DSL	0.5	26.3 ± 3.6	9.5 ± 1.4	0.36
	50	255 ± 27	117 ± 15	0.46
N90C/S407C-DSL	0.5	41 ± 1	6.7 ± 1.7	0.16
	50	706 ± 100	90 ± 13	0.13
L290C/N411C-DSL	0.5	79 ± 12	9.6 ± 1.5	0.12
	50	563 ± 36	49 ± 0	0.08

strongest inhibition by Cd^{2+} observed for the Q45C/S407C-DSL (80%), N90C/S407C-DSL (73%), and L290C/N411C-DSL (85%) mutants. When influx was measured at pH 5.5, only 35 and 20% inhibition was observed for the N90C/S407C-DSL or L290C/N411C-DSL mutants, respectively (data not shown), consistent with much weaker binding of Cd^{2+} to Cys residues at this low pH.

Impact of Folic Acid, a PCFT Substrate, on the CuPh-induced Cross-linkage between Two Cys Residues—The pairs of Cys residues, particularly, the Q45C/L290C-DSL, N90C/S407C-DSL, and L290C/N411C-DSL mutants were found to be in proximity when the mutants were unoccupied with substrates. Experiments were then undertaken to determine whether the presence of transport substrate would alter the extent of cross-linking induced by CuPh, as reflected in inhibition of transport. Folic acid was chosen in these studies as a substrate for PCFT. Preliminary data indicated that folic acid provided the greatest protection when the CuPh concentration was decreased to 1.25 μM. Among the nine double mutants studied, sufficient inhibition of activity (>40%) induced by 1.25 μM CuPh could be achieved for the Q45C/L290C-DSL, N90C/S407C-DSL, and L290C/N411C-DSL mutants. Therefore the protective effect of folic acid on the cross-link-induced inhibition was studied in these three mutants. As indicated in Fig. 6, the presence of folic acid alone did not significantly alter the activity of these mutants. CuPh at a concentration of 1.25 μM decreased the activity to 50, 55, and 40% of the control in the Q45C/L290C-DSL, N90C/S407C-DSL, and L290C/N411C-DSL mutants, respectively. The presence of folic acid during exposure to CuPh protected the activity of all three mutants. Notably, whereas CuPh inhibition (~60%) was greatest for the L290C/N411C-DSL mutant, folic acid protection was complete.

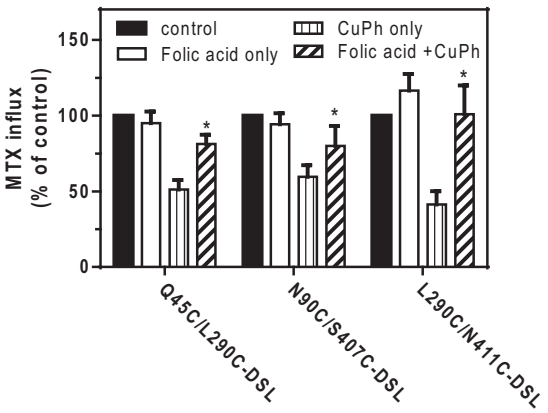

FIGURE 6. **The effect of folic acid on CuPh-induced inhibition of PCFT activity.** DTT-treated cells were incubated with 1 ml of 1.7 mM folic acid for 1 min at room temperature and then 5 min at 0 °C in HBS. An equal volume of ice-cold CuPh (2.5 μM) in HBS was added to achieve a final concentration of 0.85 mM for folic acid and 1.25 μM for CuPh. After an additional 5-min incubation at 0 °C, cells were washed three times with 0 °C HBS following which [^{3}H]MTX influx was measured (0.5 μM, pH 5.5, 1 min, 37 0 °C) immediately. Data are the mean ± S.E. from four independent experiments. The *asterisk* indicates that the increase was statistically significant as compared with the activity of cells treated with CuPh alone.

Discussion

In the absence of a crystal structure for eukaryotic solute transporters, with few exceptions (40–44), biochemical methodologies have been employed to characterize tertiary structure based upon homology models of known bacterial transporter. Cross-linking of introduced Cys pairs is an established approach to confirm the proximity of Cys-substituted residues in membrane transporters (45–47). Recently, this approach was applied to identify residues in transmembrane helices that form an extracellular or intracellular gate at external or internal interfaces of the aqueous translocation pathway based upon the inward-open or outward-open predicted structures, respectively. Hence, an extracellular gate involving two helices of the neuronal glutamate transporter EAAC1 was defined based upon the Glt_{Ph} *Pyrococcus horikoshii* glutamate transporter structure (35). Three helices of the *Leischmania donovani* nucleoside LdNT1.1 transporter were shown to form an external gate based upon an *ab initio* computational model similar to GlpT (48) as was an intracellular gate of the same transporter encompassing four different helices based upon a homology model of the *E. coli* fucose-proton symporter in the outward facing conformation (34). In the current study, a homology model of the inward-open structure of the GlpT transporter predicted helices that could be components of an extracellular gate for PCFT along with residues within those helices that appeared sufficiently close to allow the formation of a disulfide bond when substituted with a Cys moiety. The experimental data, based upon cross-linking of Cys-substituted residues in the presence and absence of the PCFT substrate along with complexing with Cd^{2+}, provide strong evidence that these four transmembrane helices are in proximity and form an extracellular gate.

Critical to the experimental design was creating a PCFT scaffold in which Cys-substituted residues only react with each other and not one of the endogenous Cys residues. Ideally, Cys-substitution studies should utilize the Cys-less transporter to exclude possible interference from native Cys residues. How-

ever, the Cys-less PCFT is vulnerable to the introduction of other mutations posing a serious limitation to the application of the substituted cysteine accessibility method (15, 33). But the preservation of only one or two native PCFT Cys residues, in an apparent nonspecific fashion, markedly reduces the vulnerability of PCFT to subsequent mutations (33). Accordingly, Cys substitutions were inserted into a disulfide bond-less PCFT (PCFT-DSL) scaffold in which both Cys^{66} and Cys^{298}, located in extracellular loops and participants in a sulfhydryl bond, were substituted with Ser. Indeed, this PCFT scaffold tolerated Q45C and L290C mutations, whereas expression of Cys-less PCFT that harbored these mutations was markedly decreased. Vulnerability of the Cys-less background to the introduction of Cys substitutions has been observed for other membrane transporters, such as *L. donovani* nucleoside transporter 1.1 (34). Hence, the method employed in this study to circumvent this problem may have broad applicability to membrane transporters, in general.

The data indicate that the substituted Cys residues in the Q45C-DSL and L290C-DSL mutants were post-translationally modified. However, this did not involve any of the native Cys residues. Post-translational modifications of a native Cys residue, primarily by *S*-glutathionylation, play a role in functional regulation of ion channels under certain physiological and pathological conditions (49). Post-translational modifications of a substituted Cys residue (T338C) were found to reduce conductance in the cystic fibrosis transmembrane conductance regulator and, under some conditions, could be reversed by DTT (36). The modification of the T338C was enhanced by the intracellular glutathione level (50), which prevented the substituted Cys from further reacting with methanethiosulfonates (51). The post-translational modification of the Cys residues introduced at positions Gln^{45} and Leu^{290} of PCFT has important ramifications for the interpretation of results based upon the substituted cysteine accessibility method in general. Hence, either the absence of biotinylation or a decrease in activity does not necessarily mean that a substituted Cys residue is not accessible to the extracellular compartment, or is not present within the aqueous translocation pathway, or is a poorly functioning transporter. Rather, it is always necessary to exclude the possibility that these properties are due to modification of the substituted Cys residue, and do not reflect its properties in its unmodified state, by evaluating the impact of pretreatment with DTT.

The following experimental results indicate that amino acid residues, Gln^{45}, Asn^{90}, Leu^{290}, Ser^{407}, and Asn^{411} of human PCFT are in proximity in the inward-open conformation predicted by the homology model. (i) There was spontaneous formation of a cross-link between N90C/S407C based upon the loss of function and lack of accessibility of the pair, both of which were reversed by treatment with DTT. (ii) There was also spontaneous formation of a disulfide bond in all double mutants containing Q45C because the slight increase in function of the Q45C single mutant induced by DTT could not account for the much greater increase in function of double mutants (Q45C/N90C-DSL, Q45C/S407C-DSL, and Q45C/N411C-DSL) that occurred with the same DTT treatment. (iii) Because the activity of the single L290C mutant could be fully restored, and the modification of the introduced Cys residues could be fully reversed by treatment with DTT, it was possible to study the impact that CuPh and Cd^{2+} had on the Cys pairs that contained this residue. Hence, the most substantial loss of function was observed for the Leu^{290}/Asn^{411} Cys pair and a lesser, although still significant loss of function, for the L290C/S407C pair. (iv) Significant loss of activity was observed for all Cys pairs containing Q45C with CuPh oxidation, and for all but Q45C/L290C with Cd^{2+}, whereas neither Q45C nor any of the other single mutants lost activity upon these treatments.

Consistent with the role of TMD-1, -2, -7, and -11 in the formation of an extracellular gate, when Cys pairs within these TMDs were cross-linked, the influx V_{max} was decreased (Table 1) indicative of a decrease in the rate of conformational change between the inward- and outward-facing transporter configurations. Furthermore, when folic acid was bound to the carrier the CuPh-induced decrease in transport for three of the Cys pairs (Fig. 6) was diminished or completely prevented. This is consistent with substrate-induced closure of the external gate resulting in decreased accessibility of the CuPh to the Cys-substituted residues as predicted by the alternating access mechanism of transport. Alternatively, as proposed for the external gate defined for the *L. donovani* nucleoside transporter 1.1, the presence of substrate may increase the distance between Cys residues during a portion of the transport cycle (48).

The formation of a disulfide bond or complex between N411C or S407C and the same residues on other helices is consistent with their positions within the context of the helix turn, the observation that both are accessible to MTSEA biotin, and the flexibility of the carrier as its oscillates between its conformational states. Although, in general, the pattern and magnitude of the effects of Cd^{2+} were comparable with the effects of CuPh, there were exceptions. The impact of Cd^{2+} on transport function was considerably less than that of CuPh for the Q45C/L290C and N90C/L290C mutants. Because Cd^{2+} should complex Cys residues further apart than occurs with a disulfide bond, this might result in less restriction of the complex and less impact on transport function. The interaction between the Cys residues appeared to be specific because the activity of all single mutants after DTT reduction was not affected by CuPh oxidation nor the presence of Cd^{2+}. This indicates further that there was no interaction between substituted Cys residues in each single mutant with any of the remaining five native Cys residues in PCFT that are located within TMD4, TMD6, TMD11, the N terminus, and the intracellular loop between TMD-8 and -9.

Author Contributions—R. Z., A. F., and I. D. G. conceived and coordinated the study and wrote the paper. R. Z. and M. N. performed the experiments. All authors analyzed the results and approved the final version of the manuscript.

References

1. Qiu, A., Jansen, M., Sakaris, A., Min, S. H., Chattopadhyay, S., Tsai, E., Sandoval, C., Zhao, R., Akabas, M. H., and Goldman, I. D. (2006) Identification of an intestinal folate transporter and the molecular basis for hereditary folate malabsorption. *Cell* **127,** 917–928

2. Visentin, M., Diop-Bove, N., Zhao, R., and Goldman, I. D. (2014) The intestinal absorption of folates. *Annu. Rev. Physiol.* **76,** 251–274
3. Diop-Bove, N., Kronn, D., and Goldman, I. D. (2014) Hereditary Folate Malabsorption. In Pagon, R. A., Adam, M. P., Ardinger, H. H., Wallace, S. E., Amemiya, A., Bean, L. J., Bird, T. D., Dolan, C. R., Fong, C. T., Smith, R. J., and Stephens, K. (eds) *GeneReviews*, University of Washington, Seattle, WA
4. Qiu, A., Min, S. H., Jansen, M., Malhotra, U., Tsai, E., Cabelof, D. C., Matherly, L. H., Zhao, R., Akabas, M. H., and Goldman, I. D. (2007) Rodent intestinal folate transporters (SLC46A1): secondary structure, functional properties, and response to dietary folate restriction. *Am. J. Physiol. Cell Physiol.* **293,** C1669-C1678
5. Unal, E. S., Zhao, R., Chang, M. H., Fiser, A., Romero, M. F., and Goldman, I. D. (2009) The functional roles of the His-247 and His-281 residues in folate and proton translocation mediated by the human proton-coupled folate transporter SLC46A1. *J. Biol. Chem.* **284,** 17846–17857
6. Umapathy, N. S., Gnana-Prakasam, J. P., Martin, P. M., Mysona, B., Dun, Y., Smith, S. B., Ganapathy, V., and Prasad, P. D. (2007) Cloning and functional characterization of the proton-coupled electrogenic folate transporter and analysis of its expression in retinal cell types. *Invest. Ophthalmol. Vis. Sci.* **48,** 5299–5305
7. Karlin, A., and Akabas, M. H. (1998) Substituted-cysteine accessibility method. *Methods Enzymol.* **293,** 123–145
8. Unal, E. S., Zhao, R., Qiu, A., and Goldman, I. D. (2008) *N*-Linked glycosylation and its impact on the electrophoretic mobility and function of the human proton-coupled folate transporter (HsPCFT). *Biochim. Biophys. Acta* **1178,** 1407–1414
9. Zhao, R., Unal, E. S., Shin, D. S., and Goldman, I. D. (2010) Membrane topological analysis of the proton-coupled folate transporter (PCFT-SLC46A1) by the substituted cysteine accessibility method. *Biochemistry* **49,** 2925–2931
10. Duddempudi, P. K., Goyal, R., Date, S. S., and Jansen, M. (2013) Delineating the extracellular water-accessible surface of the proton-coupled folate transporter. *PLoS One* **8,** e78301
11. Unal, E. S., Zhao, R., and Goldman, I. D. (2009) Role of the glutamate 185 residue in proton translocation mediated by the proton-coupled folate transporter SLC46A1. *Am. J. Physiol. Cell Physiol.* **297,** C66-C74
12. Zhao, R., Shin, D. S., Fiser, A., and Goldman, I. D. (2012) Identification of a functionally critical GXXG motif and its relationship to the folate binding site of the proton-coupled folate transporter (PCFT-SLC46A1). *Am. J. Physiol. Cell Physiol.* **303,** C673-C681
13. Shin, D. S., Zhao, R., Yap, E. H., Fiser, A., and Goldman, I. D. (2012) A P425R mutation of the proton-coupled folate transporter causing hereditary folate malabsorption produces a highly selective alteration in folate binding. *Am. J. Physiol. Cell Physiol.* **302,** C1405-C1412
14. Shin, D. S., Zhao, R., Fiser, A., and Goldman, I. D. (2013) The role of the fourth transmembrane domain in proton-coupled folate transporter (PCFT) function as assessed by the substituted cysteine accessibility method. *Am. J. Physiol. Cell Physiol.* **304,** C1159-C1167
15. Wilson, M. R., Hou, Z., and Matherly, L. H. (2014) Substituted cysteine accessibility reveals a novel transmembrane 2–3 reentrant loop and functional role for transmembrane domain 2 in the human proton-coupled folate transporter. *J. Biol. Chem.* **289,** 25287–25295
16. Zhao, R., Min, S. H., Qiu, A., Sakaris, A., Goldberg, G. L., Sandoval, C., Malatack, J. J., Rosenblatt, D. S., and Goldman, I. D. (2007) The spectrum of mutations in the PCFT gene, coding for an intestinal folate transporter, that are the basis for hereditary folate malabsorption. *Blood* **110,** 1147–1152
17. Shin, D. S., Min, S. H., Russell, L., Zhao, R., Fiser, A., and Goldman, I. D. (2010) Functional roles of aspartate residues of the proton-coupled folate transporter (PCFT; SLC46A1); a D156Y mutation causing hereditary folate malabsorption. *Blood* **116,** 5162–5169
18. Mahadeo, K., Diop-Bove, N., Shin, D., Unal, E. S., Teo, J., Zhao, R., Chang, M. H., Fulterer, A., Romero, M. F., and Goldman, I. D. (2010) Properties of the Arg376 residue of the proton-coupled folate transporter (PCFT-SLC46A1) and a glutamine mutant causing hereditary folate malabsorption. *Am. J. Physiol. Cell Physiol.* **299,** C1153-C1161
19. Shin, D. S., Zhao, R., Fiser, A., and Goldman, D. I. (2012) Functional roles of the A335 and G338 residues of the proton-coupled folate transporter (PCFT-SLC46A1) mutated in hereditary folate malabsorption. *Am. J. Physiol. Cell Physiol.* **303,** C834-C842
20. Lasry, I., Berman, B., Glaser, F., Jansen, G., and Assaraf, Y. G. (2009) Hereditary folate malabsorption: a positively charged amino acid at position 113 of the proton-coupled folate transporter (PCFT/SLC46A1) is required for folic acid binding. *Biochem. Biophys. Res. Commun.* **386,** 426–431
21. Lasry, I., Berman, B., Straussberg, R., Sofer, Y., Bessler, H., Sharkia, M., Glaser, F., Jansen, G., Drori, S., and Assaraf, Y. G. (2008) A novel loss of function mutation in the proton-coupled folate transporter from a patient with hereditary folate malabsorption reveals that Arg 113 is crucial for function. *Blood* **112,** 2055–2061
22. Visentin, M., Unal, E. S., Najmi, M., Fiser, A., Zhao, R., and Goldman, I. D. (2015) Identification of Tyr residues that enhance folate substrate binding and constrain oscillation of the proton-coupled folate transporter (PCFT-SLC46A1). *Am. J. Physiol. Cell Physiol.* **308,** C631-C641
23. Zhao, R., Gao, F., Hanscom, M., and Goldman, I. D. (2004) A prominent low-pH methotrexate transport activity in human solid tumor cells: contribution to the preservation of methotrexate pharmacological activity in HeLa cells lacking the reduced folate carrier. *Clin. Cancer Res.* **10,** 718–727
24. Diop-Bove, N. K., Wu, J., Zhao, R., Locker, J., and Goldman, I. D. (2009) Hypermethylation of the human proton-coupled folate transporter (SLC46A1) minimal transcriptional regulatory region in an antifolate-resistant HeLa cell line. *Mol. Cancer Ther.* **8,** 2424–2431
25. Zhao, R., Chattopadhyay, S., Hanscom, M., and Goldman, I. D. (2004) Antifolate resistance in a HeLa cell line associated with impaired transport independent of the reduced folate carrier. *Clin. Cancer Res.* **10,** 8735–8742
26. Sippl, M. J. (1993) Recognition of errors in three-dimensional structures of proteins. *Proteins* **17,** 355–362
27. Hildebrand, A., Remmert, M., Biegert, A., and Söding, J. (2009) Fast and accurate automatic structure prediction with HHpred. *Proteins* **77,** 128–132
28. Fernandez-Fuentes, N., Madrid-Aliste, C. J., Rai, B. K., Fajardo, J. E., and Fiser, A. (2007) M4T: a comparative protein structure modeling server. *Nucleic Acids Res.* **35,** W363-W368
29. Fernandez-Fuentes, N., Rai, B. K., Madrid-Aliste, C. J., Fajardo, J. E., and Fiser, A. (2007) Comparative protein structure modeling by combining multiple templates and optimizing sequence-to-structure alignments. *Bioinformatics* **23,** 2558–2565
30. Rai, B. K., and Fiser, A. (2006) Multiple mapping method: a novel approach to the sequence-to-structure alignment problem in comparative protein structure modeling. *Proteins* **63,** 644–661
31. Rai, B. K., Madrid-Aliste, C. J., Fajardo, J. E., and Fiser, A. (2006) MMM: a sequence-to-structure alignment protocol. *Bioinformatics* **22,** 2691–2692
32. Tusnády, G. E., and Simon, I. (1998) Principles governing amino acid composition of integral membrane proteins: application to topology prediction. *J. Mol. Biol.* **283,** 489–506
33. Zhao, R., Shin, D. S., and Goldman, I. D. (2011) Vulnerability of the cysteine-less proton-coupled folate transporter (PCFT-SLC46A1) to mutational stress associated with the substituted cysteine accessibility method. *Biochim. Biophys. Acta* **1808,** 1140–1145
34. Valdés, R., Elferich, J., Shinde, U., and Landfear, S. M. (2014) Identification of the intracellular gate for a member of the equilibrative nucleoside transporter (ENT) family. *J. Biol. Chem.* **289,** 8799–8809
35. Shabaneh, M., Rosental, N., and Kanner, B. I. (2014) Disulfide cross-linking of transport and trimerization domains of a neuronal glutamate transporter restricts the role of the substrate to the gating of the anion conductance. *J. Biol. Chem.* **289,** 11175–11182
36. Liu, X., Alexander, C., Serrano, J., Borg, E., and Dawson, D. C. (2006) Variable reactivity of an engineered cysteine at position 338 in cystic fibrosis transmembrane conductance regulator reflects different chemical states of the thiol. *J. Biol. Chem.* **281,** 8275–8285
37. Bénitah, J. P., Tomaselli, G. F., and Marban, E. (1996) Adjacent pore-lining residues within sodium channels identified by paired cysteine mutagenesis. *Proc. Natl. Acad. Sci. U.S.A.* **93,** 7392–7396
38. Zhao, R., Hanscom, M., Chattopadhyay, S., and Goldman, I. D. (2004)

Selective preservation of pemetrexed pharmacological activity in HeLa cells lacking the reduced folate carrier; association with the presence of a secondary transport pathway. *Cancer Res.* **64,** 3313–3319
39. Zhao, R., Qiu, A., Tsai, E., Jansen, M., Akabas, M. H., and Goldman, I. D. (2008) The proton-coupled folate transporter (PCFT): impact on pemetrexed transport and on antifolate activities as compared to the reduced folate carrier. *Mol. Pharmacol.* **74,** 854–862
40. Pedersen, B. P., Kumar, H., Waight, A. B., Risenmay, A. J., Roe-Zurz, Z., Chau, B. H., Schlessinger, A., Bonomi, M., Harries, W., Sali, A., Johri, A. K., and Stroud, R. M. (2013) Crystal structure of a eukaryotic phosphate transporter. *Nature* **496,** 533–536
41. Parker, J. L., and Newstead, S. (2014) Molecular basis of nitrate uptake by the plant nitrate transporter NRT1.1. *Nature* **507,** 68–72
42. Sun, J., Bankston, J. R., Payandeh, J., Hinds, T. R., Zagotta, W. N., and Zheng, N. (2014) Crystal structure of the plant dual-affinity nitrate transporter NRT1.1. *Nature* **507,** 73–77
43. Deng, D., Sun, P., Yan, C., Ke, M., Jiang, X., Xiong, L., Ren, W., Hirata, K., Yamamoto, M., Fan, S., and Yan, N. (2015) Molecular basis of ligand recognition and transport by glucose transporters. *Nature* **526,** 391–396
44. Penmatsa, A., Wang, K. H., and Gouaux, E. (2013) X-ray structure of dopamine transporter elucidates antidepressant mechanism. *Nature* **503,** 85–90
45. Mueckler, M., and Makepeace, C. (2012) Ligand-induced movements of inner transmembrane helices of Glut1 revealed by chemical cross-linking of di-cysteine mutants. *PLoS One* **7,** e31412
46. Hilwi, M., Dayan, O., and Kanner, B. I. (2014) Conformationally sensitive proximity of extracellular loops 2 and 4 of the gamma-aminobutyric acid (GABA) transporter GAT-1 inferred from paired cysteine mutagenesis. *J. Biol. Chem.* **289,** 34258–34266
47. Loo, T. W., and Clarke, D. M. (2014) Cysteines introduced into extracellular loops 1 and 4 of human P-glycoprotein that are close only in the open conformation spontaneously form a disulfide bond that inhibits drug efflux and ATPase activity. *J. Biol. Chem.* **289,** 24749–24758
48. Valdés, R., Shinde, U., and Landfear, S. M. (2012) Cysteine cross-linking defines the extracellular gate for the *Leishmania donovani* nucleoside transporter 1.1 (LdNT1.1). *J. Biol. Chem.* **287,** 44036–44045
49. Yang, Y., Jin, X., and Jiang, C. (2014) S-glutathionylation of ion channels: insights into the regulation of channel functions, thiol modification crosstalk, and mechanosensing. *Antioxid. Redox Signal.* **20,** 937–951
50. Liu, X. (2008) A possible role for intracellular GSH in spontaneous reaction of a cysteine (T338C) engineered into the cystic fibrosis transmembrane conductance regulator. *Biometals* **21,** 277–287
51. Cheung, M., and Akabas, M. H. (1996) Identification of cystic fibrosis transmembrane conductance regulator channel-lining residues in and flanking the M6 membrane-spanning segment. *Biophys. J.* **70,** 2688–2695